Predicting the deleterious effects of mutation load in fragmented populations

J. Jaquiéry[1, §], F. Guillaume[2, §] and N. Perrin[1]

[1)] Department of Ecology and Evolution, University of Lausanne, CH-1015 Lausanne, Switzerland

[2)] Department of Zoology, University of British Columbia, Vancouver, B.C., Canada

[§)] These authors contributed equally to this work.

Corresponding author: Julie Jaquiéry, Department of Ecology and Evolution, University of Lausanne, CH-1015 Lausanne, Switzerland

e-mail: Julie.Jaquiery@unil.ch

Tel.: ++ 41 21 692 41 76

Intended as a contributed paper for *Conservation Biology*

Running head: Viability in fragmented populations

Word count: 5968

Keywords: Offspring viability, metapopulation, mutation load, genetic structure, extinction time, habitat fragmentation

ABSTRACT

Human-induced habitat fragmentation constitutes a major threat to biodiversity. Both genetic and demographic factors combine to drive small and isolated populations into extinction vortices. However, the deleterious effects of inbreeding and drift load may depend on population structure, migration patterns and mating systems, and are difficult to predict in the absence of crossing experiments. We performed stochastic individual-based simulations aimed at predicting the effects of deleterious mutations on population fitness (offspring viability and median time to extinction) under a variety of settings (landscape configurations, migration models, and mating systems) on the basis of easy-to-collect demographic and genetic information. Pooling all simulations, a large part (70%) of variance in offspring viability was explained by a combination of genetic structure (F_{ST}) and within-deme heterozygosity (H_S). A similar part of variance in median time to extinction was explained by a combination of local population size (N) and heterozygosity (H_S). In both cases, the predictive power increased above 80% when information on mating systems was available. These results provide robust predictive models to evaluate the viability prospects of fragmented populations.

INTRODUCTION

Human-induced habitat fragmentation constitutes a major threat for biodiversity (Frankham 1995). Consequences are, at first, demographic. Small and isolated populations suffer from increased stochasticity and limited rescue effects, which may suffice to cause local extinctions (Lande 1993; Hanski & Ovaskainen 2000). But fragmentation also has genetic consequences, which are likely to contribute significantly to extinction risks. Increased genetic drift reduces the effectiveness of selection against deleterious mutations (Kimura et al. 1963), leading to their progressive accumulation (e.g., Lynch et al. 1995), and decreases both the standing genetic variation and the rate of fixation of beneficial mutations (Whitlock 2003), limiting the evolutionary potential of isolated populations. Although the importance of genetic relative to demographic factors is still debated (e.g., Frankham 1995; Lande 1995; Spielman et al. 2004), the 2 factors are expected to interact and feed back on each other, progressively driving fragmented populations into "extinction vortices" (Lacy & Lindenmayer 1995) or "mutational melt-downs" (Lynch et al. 1995; Higgins & Lynch 2001).

The potential effects of deleterious mutations on population fitness are often estimated from the level of inbreeding load. Assuming a negative exponential relationship between fitness and inbreeding coefficient of individuals within a population (Morton et al. 1956; Kalinowski & Hedrick 1998), the slope of the regression of log(fitness) against inbreeding coefficient provides an estimate of inbreeding load, or number of lethal equivalents (reviewed in Keller & Waller 2002). Inbreeding load in wild populations is commonly high (e.g., Ralls et al. 1988; Kruuk et al. 2002; Reed et al. 2007) although exceptions exist (e.g. Duarte et al. 2003).

Viability losses, however, may also come from drift load, i.e. the local fixation of mild deleterious mutations hidden from selection by drift (Keller & Waller 2002). Small

63 populations are actually expected to harbour more drift load (Whitlock et al. 2000) and less
64 inbreeding load than large ones (because individuals are genetically more similar locally; e.g.,
65 Bataillon & Kirkpatrick 2000). Local drift load is not revealed by regression of fitness on
66 inbreeding coefficient but by heterosis effects (i.e., fitness increase of offspring from crosses
67 among compared to within populations), and has also received wide empirical support (e.g.,
68 Coulson et al. 1998; Marr et al. 2002; Bush 2006). Since local populations may exhibit low
69 inbreeding load but high drift loads, management decisions made on the basis of inbreeding
70 depression only may be misleading.
71 Although the dramatic consequences of both inbreeding and drift loads have been
72 recognized, there is no simple way to incorporate them in the toolbox of conservation
73 geneticists without turning to heavy experimental designs (within and between population
74 crosses). Keller and Waller (2002) suggest use of F_{ST} as "an index of the susceptibility of a
75 population to the deleterious effects of drift load". Whitlock (2002) showed that the local drift
76 load caused by mild deleterious mutations may indeed increase with F_{ST} in an infinitely large
77 metapopulation, depending on the mode of population regulation and mutation parameters.
78 Using stochastic individual-based simulations, Higgins and Lynch (2001) showed
79 metapopulation viability increases with the number, size, and connectivity of local demes.
80 Theodorou and Couvet (2006) further showed that, for a given metapopulation size, fitness is
81 higher with a few large populations than with several small ones, and that for small, isolated
82 populations the increase in local population size has a much greater positive effect on
83 population fitness than other parameters, such as migration or number of demes.
84 The effect of connectivity was formalized by the one-migrant-per-generation (OMPG)
85 rule, according to which one migrant per generation should suffice to protect local
86 populations from the accumulation of deleterious mutations (e.g., Mills & Allendorf 1996;
87 Couvet 2002; Wang 2004). However, migration rate is notoriously difficult to assess in the

field (Whitlock & McCauley 1999), and its effect may depend on other parameters such as migration model, total metapopulation size, and mating system, which affects the purging of deleterious mutations (Glémin 2003).

In the present study, we used stochastic individual-based simulations to investigate population fitness (offspring viability and time to extinction) under various metapopulation settings. The aims were (1) to derive robust predictive models of population fitness from easy-to-collect genetic and demographic data that may account for both inbreeding and drift loads, and (2) to test the validity of the OMPG rule under different migration models and mating systems.

METHODS

Life cycle

We performed simulations in Nemo, a stochastic, individual-based, genetically-explicit framework (Guillaume & Rougemont 2006). Model organisms were diploid, with separate genders or not depending on the mating system, and lived in a structured metapopulation of d demes with local carrying capacity, N. A series of loci were subject to deleterious mutations, whereas others were neutral. We implemented the following semelparous life cycle: (1) viability selection on newly-born offspring that survived with a probability derived from their deleterious mutation genotype; (2) dispersal of surviving offspring according to a specific migration model (see below); (3) random regulation of local populations, which reduced the pool of competing individuals to the local carrying capacity (with equal sex ratios in case of separate genders); (4) reproduction during which females were assigned a fecundity value drawn from a Poisson distribution with constant mean f and were mated as many times as indicated by their fecundity (one offspring per mating). Males were chosen according to 1 of

112 the 3 mating systems described below (random mating, selfing, or polygyny). Offspring
113 alleles at neutral and selected loci were inherited randomly (i.e., no linkage), baring
114 mutations. Sex was set randomly (with equal sex ratio) when genders were distinct. Adults
115 were removed after reproduction, and the cycle started again.
116
117 *Population structure, dispersal, and mating system*
118 We ran simulations under different metapopulation configurations to cover a large range of
119 fragmentation levels. We varied independently local (N=4, 8, 16, 25, 50, and 100 individuals)
120 and total metapopulation sizes (N_t=200, 400, 800, and 1600). The number of demes (d) was
121 set by the ratio $d=N_t/N$. For each metapopulation configuration, we used 4 different migration
122 rates (m=0.001, 0.003, 0.01, and 0.1) and 2 different migration models (island and linear
123 stepping stone) that represented the 2 extremes of a continuum of isolation by distance. Most
124 realistic cases are likely to fall in-between. The effect of systematic inbreeding induced by
125 mating patterns was explored with 3 systems: random mating, selfing, and polygyny. Selfing
126 rate was set to 50%, the other 50% resulted from random mating within the deme. Under
127 polygyny, only one-quarter of the males present in each population were allowed to
128 reproduce, so successful males mated on average with 4 females.
129 We thus obtained a fully-factorial core set of simulations exploring 576 parameter
130 combinations (6 local population sizes, 4 total population sizes, 4 migration rates, 2 migration
131 models, 3 mating systems). The 6 combinations of mating systems and migration models will
132 be referred to as datasets 1 to 6. For this core set, average fecundity f was set to 15 for females
133 (random mating and polygyny) and 7.5 for hermaphrodites (selfing) in order to keep the same
134 reproductive output per population. The effect of lowered fecundity (f=6) was investigated
135 under random mating and island migration in an additional set of simulations (dataset 7).
136

Mutation models

The neutral markers, used to assess the level of neutral genetic diversity within and among populations, followed a *k*–allele mutation model (KAM), with k=256 possible allelic states over each of 24 loci and a mutation rate u=0.0001.

Fitness was controlled by a set of L (fixed to 1000) independent loci carrying deleterious alleles of various strength and dominance effect. We drew the number of new mutations occurring in a particular genome from a Poisson distribution with mean equal to the diploid genomic mutation rate (U). Mutations affected only nondeleterious alleles, turning them into the deleterious form (reverse mutations were neglected), and acted independently on fitness so that offspring viability (v) was computed as the product of fitness at each locus i: $v=\Pi_L\, v_i$, where v_i is 1, $1 - s_i$ or $1 - h_i s_i$ if the locus was homozygous wild-type, homozygous mutant, or heterozygous, respectively. The values used for the mean mutation effect ($\bar{s}$ =0.05) and average dominance ($\bar{h}$ =0.36) were derived from *Drosophila* studies (reviewed in Lynch et al. 1999) and are commonly used in simulations (Wang et al. 1999; Higgins & Lynch 2001; Theodorou & Couvet 2006).

For the core set of simulations, the genomic mutation rate was fixed to U=0.5, and the mutant effects s were exponentially distributed among the L loci. Following Wang et al. (1999), the dominance coefficient h of a mutation with effect s was set to satisfy the relationship $h=\exp(-ks)/2$, where k is a constant chosen so that the average dominance of all mutations in the genome equals $\bar{h}$ (Caballero & Keightley 1994). This induced an inverse relationship between the magnitude of effect of a mutation and its degree of dominance, as expected from biochemical arguments and supported by mutation accumulation experiments (Simmons & Crow 1977; Phadnis & Fry 2005).

We also performed additional simulations under random mating and island migration

to further explore the effects of genomic mutation rate (U=1, dataset 8) and the distributions of deleterious effects, assuming either a truncated log-normal (dataset 9) or a gamma distribution (dataset 10). The log-normal was parameterized according to Loewe and Charlesworth (2006) with log-mean = -6.4 and log-stdev = 5.3. The distribution was truncated to the right to have no s >1 (and $\bar{s}$ =0.05). The shape parameter for the gamma distribution (α=1.69374) was taken from Keightley's (1994) estimation on the Mukai et al. (1972) *Drosophila* dataset, and its scale adjusted to have $\bar{s}$ =0.05.

Simulations

For each of the 960 combinations of parameters (576 for the core set plus 384 for the 4 additional sets), we first performed 30 replicates over 50,000 generations with neutral markers only (in order to get the required statistics for parameter values that would lead to population crashes in the presence of deleterious mutations), then 15 replicates over 5000 generations after adding deleterious-mutations effects. At the start of simulations, neutral markers were assigned random allelic values to insure a maximal initial variance, and loci under selection were fixed to the fit allele. Statistics were recorded every 10 generations and measured from the offspring that survived the viability selection episode.

Statistical analyses

We computed mean F_{ST}, H_O, H_S, and H_T (Nei & Chesser 1983), first over the 30 neutral replicates (averaged over generations 20,000 to 50,000), second over the 15 replicates with deleterious mutations (generations 4,500 to 5,000), together with offspring viability v (for simulations in which all 15 replicates survived) and median time to extinction MTE (for simulations in which more than 50% of the replicates crashed before 5000 generations).

185 To find the best predictors of offspring viability from the core dataset we proceeded in
186 3 steps. First, we transformed the potential predictors (F_{ST}, H_O, H_S, H_T, d, N, and N_t) with the
187 functions x, log(x), 1/x, and 1/log(x), as well as log(1-x) for predictors ranging from 0 to 1,
188 and selected the transformations providing the best linear relationship with logit(viability)
189 ($=\log\frac{v}{1-v}$). These turned out to be log(1-F_{ST}), log(H_O), log(H_S), H_T, log(N_t), log(N), and
190 log(d).
191 Second, we performed linear regressions of logit(viability) on the transformed
192 predictors for each mating system and migration model independently (hence, 6 partitions).
193 The same analyses were performed on data pooled by mating system (3 partitions), migration
194 models (2 partitions) and then on the entire data set.
195 Third, we combined predictors 2 by 2 ($y \sim ax1 + bx2 + c$) to find the best bivariate
196 prediction of logit (viability) on the same partitions as above. The different models were then
197 ranked on the basis of the amount of explained variance, and ranks were averaged to select the
198 best overall model.
199 We used the same procedure to predict median time to extinction from the core dataset
200 (with 1/MTE as the dependent variable), and to analyze the additional simulations (datasets 7
201 to 10). We did not perform multiple stepwise regressions, which, owing to the high power of
202 simulation studies, tend to retain too many variables, and usually different ones depending on
203 the settings (data not shown).
204
205 ## RESULTS
206 Genetic parameters calculated on neutral markers (F_{ST}, H_O, H_S, and H_T) did not differ
207 whether calculated in the presence or absence of deleterious mutations (correlation
208 coefficients ranging 0.97 to 0.99); thus, we consider only values in absence of mutation load

hereafter. The F_{ST} averaged 0.68 (range 0.007 to 0.995), H_O=0.07 (range 0.003 to 0.38), H_S=0.08 (range 0.004 to 0.38), and H_T=0.49 (range 0.03 to 0.98). Spearman rank correlation between the predictors ranged from -0.87 to 0.97 (Table 1).

Offspring viability

Over the surviving populations from the core dataset, offspring viability averaged 43%, depending greatly on the mating system and slightly on the migration model. It was highest under self-fertilization (averaging 49% and 45% for the island- and stepping-stone models of migration) but had a wide range (19% to 68%). Values were slightly lower under random mating (45% and 43% respectively, range 23% to 59%) and lowest under polygyny (37% and 33% respectively, range 18% to 56%).

Offspring viability was well predicted by $\log(H_S)$, $\log(1-F_{ST})$, and $\log(H_O)$, with 41% to 67% of the variance explained depending on the partition used, but none of them ranking systematically higher (average ranking 1.7, 2.0 and 2.3, respectively). All 3 descriptors still explained at least 46% of variance when pooling data by mating system, but $\log(H_O)$ lost explanatory power when data were pooled by migration model (R^2<31%). When pooling all 6 partitions, $\log(H_S)$ and $\log(1-F_{ST})$ remained the best predictors (R^2=46% and 42%, respectively).

Both were also included in the best bivariate combination (Table 2), with an average rank of 1.0 (i.e., best in all cases). When pooling all 6 partitions, 70% of variance (Table 2) was explained by:

$$\log\frac{v}{1-v} = a\log(1-F_{ST}) + b\log(H_S) + c \quad , \qquad (1)$$

with a=0.39, b=0.52, and c=1.19. The explained variance increased to 71-74% when splitting data by migration models (2 partitions), 87-92% when splitting by mating system (3

partitions), and 90-97% when simultaneously splitting by migration model and mating system (6 partitions; Table 2). Regression coefficients were positive in all cases, but viability displayed a sharper transition from high to low values under selfing than under polygyny or random mating (Fig.1). Simulations that collapsed because of mutational meltdown fell well within the predicted low-viability area, even though these data were not used for model fitting.

Decreasing fecundity (f=6, dataset 7) had no effect on offspring viability, and model (1) explained 85% of variance (Table 2). Increasing mutation rate (U=1, dataset 8) lowered offspring viability, but model (1) remained excellent (rank 2; R^2=93%). The log-normal and gamma distributions of deleterious effects (datasets 9 and 10) had only marginal effects on offspring viability, and model (1) also remained the best (rank 1 in both cases), with 95% and 87% of variance explained respectively (Table 2).

Time to extinction

Extinction rate averaged 51% over the core dataset (294 out of 576 simulations were extinct before 5000 generations) and was higher under polygyny (70%) than under random mating (45%) or selfing (38%). It was also higher under the stepping-stone dispersal (76%, 50%, and 43% for polygyny, random mating, and selfing respectively) than under island model (67%, 40% and 32% respectively).

Median time to extinction (MTE) did not differ much among mating systems (averages 1079, 1118, and 1137 generations under polygyny, random mating, and selfing respectively), with similar ranges (200 to 4000 generations). The 1/MTE correlated mainly with log(1-F_{ST}), log(H_S), log(H_O), and log(N) (with R^2 ranging from 22% to 83%), but none of these variables showed consistency among the different models. Accordingly, model ranks were very similar (2.2, 2.3, 3, and 3.2 for log[1-F_{ST}], log[H_S], log[N], and log[H_O]

258 respectively). After pooling all data, log(1-F_{ST}) and log(N) remained the best candidates
259 (R^2=50% and 49%, respectively), followed by log(H_S) (R^2=43%).
260 When pooling all 6 partitions, the best bivariate model for predicting extinction time
261 combined log(H_S) and log(N):
262 $$1/\mathrm{MTE} = a\log(H_S) + b\log(N) + c, \quad (2)$$
263 with a= -8.36 10^{-4}, b= -8.30 10^{-4}, and c=7.65 10^{-4} (R^2=68%; Table 3). The same model
264 emerged when considering the average ranking over the different partitions (rank 2.2; the
265 second-best model was 1/MTE ~log[N_t] + log[H_O] with rank 2.8). The explained variance
266 reached 66-81% when splitting data by migration models (2 partitions), 81-86% when
267 splitting by mating system (3 partitions), and 79-97% when simultaneously splitting for
268 migration model and mating system (6 partitions; Table 3). Regression coefficients were
269 negative in all cases (Table 3 and Fig.2). Metapopulations still viable at generation 5000 fell
270 well within the predicted viable area, even though these data were not used for model fitting.
271 The model (2) was also good to predict median time to extinction in simulation runs
272 with f=6, U=1, and log-normal or gamma distribution of deleterious effects (average rank
273 about 3), with 73-94% of the variance explained (Table 3).
274
275 *Inbreeding and purge of the genetic load*
276 The ratio of offspring viability under selfing or polygyny relative to random mating was used
277 to assess the extent of the purge in either of these mating systems. The ratio consistently
278 exceeded unity in selfing populations (1.167 $\pm$ 0.136 SD), which had thus purged part of their
279 mutational load. Polygynous populations underwent a higher rate of accumulation of
280 deleterious mutations than under random mating (ratio 0.656 $\pm$ 0.168), inducing the higher
281 extinction rates noted above. Note however that F_{IS} was not retained as a good predictor for

offspring viability or time to extinction in the regression analyses (data not shown).

One-migrant-per-generation rule

For both random mating and selfing, one migrant per population per generation was enough to allow metapopulation persistence under our core settings (Fig.3b and c). None of the simulations where effective migration rate (N_m) exceeded 1 went extinct, and there were only a handful for N_m values between 0.1 and 1 (4 under selfing and 9 under random mating), occurring under small local populations sizes (N=4 to 16) and low connectivity (stepping-stone dispersal). Under polygyny by contrast, extinctions occurred for N_m values exceeding 1, but only at small metapopulation sizes (N_t=200). Lower fecundity values (f=6, Fig.3d) did not affect offspring viability, but increased the threshold value below which populations are at risk. Extinctions occurred for N_m values exceeding 1, but only when both total and local populations sizes were small (N_t=200 and N<100). A higher genomic mutation rate (U=1, Fig.3e) decreased offspring viability, so that extinctions occurred for N_m values exceeding 1, but only for small metapopulation sizes (N_t=200).

DISCUSSION

On the basis of our results, the effects of deleterious mutations on population fitness can be largely accounted for by a few basic genetic and demographic measurements. Offspring viability increased with genetic diversity within demes (H_S) and decreased with differentiation among them (F_{ST}), in line with both analytical treatments (Kimura et al. 1963; Whitlock et al. 2000; Whitlock 2002) and empirical observations (e.g., Madsen et al. 1996; Newman & Pilson 1997; Saccheri et al. 1998). On its own, F_{ST} explained 42% of the variance in offspring viability over our core dataset, corroborating Whitlock's (2002) analytical results under infinite-island settings and supporting Keller and Waller's (2002) suggestion that

307 F_{ST} be used as "an index of the susceptibility of a population to the deleterious effects of drift
308 load". The positive role of diversity (H_S), on the other hand, more likely resulted from the
309 deleterious effect of inbreeding load. A combination of both H_S and F_{ST} accounted for both
310 loads and thus explained a large part of the variance in offspring viability (R^2>85% for a
311 given mating system).

312 The median time to extinction also increased with diversity within demes (H_S), but the
313 best bivariate regression included local population size (N), rather than F_{ST}, in addition to H_S
314 (with R^2>80% for a given mating system). This point underlines the importance of both
315 demographic and genetic effects during the process of mutational meltdown, in line with both
316 analytical models (Lande 1994; Lynch et al. 1995) and empirical observations (e.g., Saccheri
317 et al. 1988). Small population sizes are known to enhance both demographic and genetic
318 stochasticity, with positive feedbacks. Populations collapsed at offspring viability values
319 below 0.2 for f=15 (and below 0.4 for f=6; Fig.3), corresponding to effective reproductive
320 rates exceeding unity, which, in absence of stochasticity, should allow positive growth rate
321 and population persistence. This illustrates the initiation of extinction vortices by the interplay
322 between demographic and genetic factors as soon as the system enters a critical state in terms
323 of population size and mutation load.

324 Local population size was not retained in offspring viability models, contrasting with
325 empirical support for a positive correlation between population size and fitness (reviewed in
326 Reed 2005; see also Reed et al. 2007). Local size certainly affects a population's ability to
327 resist drift, but our simulations also included other factors that drastically affect local genetic
328 diversity (mating system, migration rate, and total metapopulation size). Population fitness
329 and genetic diversity should depend more on local *effective* size, which may present only
330 weak correlations with *census* size when such interacting factors are varied. Mating systems
331 also had an effect of their own in lowering the relationship between population size and

offspring viability, since selfing, which reduces effective size, increased fitness by purging the genetic load. Selection is more efficient at removing deleterious mutations under such mixed systems than under random mating, due to increased variance in individual fitness and inbreeding coefficients (see Glémin 2003 for an analytical treatment). Under polygyny, by contrast, both the effective population size and variance in inbreeding were reduced, leading to a greater rate of mutation accumulation and population extinction.

Total population size (N_t) also played a significant role in our simulations because the dynamics of local genetic diversity within demes also depends on inputs from the metapopulation reservoir. Depending on the mating system, 53% to 78% of the variance in H_S was explained by $\log(N_t)$. In small metapopulations ($N_t \leq 800$), furthermore, deleterious mutations may get fixed at the global scale, with long-lasting consequences on population fitness via drift load, but without contributing to inbreeding depression or heterosis anymore (see also Whitlock 2002). Metapopulations of 200 individuals were often too small to persist, owing to dramatically low offspring viabilities, whatever the connectivity (Fig.1 and 3). These effects have been poorly investigated until now, mainly because analytical treatments usually assume infinite or very large metapopulations (e.g., Whitlock 2002) and that previous simulations studies have not addressed variance in this parameter (Higgins & Lynch 2001; Theodorou & Couvet 2006).

Our results rejoin these 2 latter studies with respect to the effects of fragmentation. For the same total number of individuals (and no environmental stochasticity), one big population was better than several small. Doubling the number of populations was much less efficient than doubling the size of local populations. Increasing connectivity was quite efficient, provided that the total population size was not too small (>500) and that local populations were smaller than 100 individuals. We thus emphasize the importance for persistence of connecting isolated populations to a reservoir of genetic diversity.

Our results also provide some validation for the OMPG rule, with some caveats however. As shown in Fig.3, populations did not collapse for effective numbers of immigrant exceeding one under most parameter values. Exceptions occurred only for very small metapopulation sizes (N_t=200), and only in conjunction with other negative effects such as polygyny (Fig.3a), low fecundity (Fig.3d) or high genomic deleterious mutation rate (Fig.3e).

Migration rates and population sizes were deliberately set to low values in order to simulate endangered populations, usually characterized by small global sizes (<2500 individuals, World Conservation Union 2001) and reduced connectivity. As a result, about half of the simulations collapsed due to mutational meltdown (whereas the persisting ones presented a large range of viability values), and population structure (F_{ST}) sometimes reached values close to unity. This obviously exceeds the values usually documented in natural situations because most situations fall within the range of 0 to 0.2 (Morjan & Rieseberg 2004). However, endangered populations frequently display F_{ST} values exceeding 20% (e.g., Rowe et al. 2000; Eckstein et al. 2006; Kawamura et al. 2007). Moreover, the F_{ST} values measured for most of recently fragmented and/or bottlenecked populations are likely to be underestimates because these populations usually have not had enough time to reach genetic equilibrium (Whitlock 1992; Wang 2004). We thus covered a wide panel of population genetic structures within which most endangered species are expected to fall.

One important point to emphasize is that our results must not be considered in quantitative (absolute) terms, but only in qualitative (relative) terms, owing to the specificity of several assumptions underlying our simulations. This caveat obviously applies to our life-history assumptions. Lower fecundities, in particular, increase the viability threshold under which extinctions occur (Fig.3d), even though models 1 and 2 still hold qualitatively. Also, the genetic variance at neutral markers depends not only on effective sizes, but also on mutation rates, which might be species-specific and difficult to estimate precisely.

382 Similarly, the mutation model and parameters values used in our core simulations come from
383 accumulation experiments performed on a single model organism, *Drosophila* (Simmons &
384 Crow 1977; Lynch et al. 1999). Although our conclusions seem quite robust regarding the
385 distribution of deleterious mutations (Fig.3c), parameter values may vary among species. The
386 genomic mutation rate in particular quantitatively affected expectations (Fig.3e), even though
387 models 1 and 2 still hold qualitatively. Our results will be therefore best used in a comparative
388 context, e.g. to rank the effects of different management strategies for a given endangered
389 species. The conservation value of different scenarios can be evaluated on the basis of their
390 effect on a set of very few key genetic and demographic parameters (H_S, F_{ST}, and N). More
391 specific questions might also be addressed with the same simulation framework (Nemo;
392 Guillaume & Rougemont 2006), or, if empirical data are available, by directly evaluating
393 regression coefficients of offspring viability on the relevant variables (i.e., H_S, F_{ST}, and N).
394 Our approach also bears a series of important advantages. First, it provides robust
395 predictive models with which to assess the viability prospects of fragmented populations,
396 which might usefully complement the OMPG rule (e.g., Frankel & Soulé 1981; Mills &
397 Allendorf 1996; Wang 2004) since assessing migration rates in nature is still a major
398 challenge in ecology (Whitlock & McCauley 1999), which often precludes its effective use.
399 Second, predictive power is large even without specific information on the mating system or
400 dispersal model ($R^2 \approx 70\%$ on pooled data) and increases with additional information on the
401 mating system ($R^2 > 80\%$). Third, no lab breeding or controlled crosses are needed to estimate
402 inbreeding or drift load, which are both difficult or impossible to carry out on threatened
403 species. The genetic information required is readily obtained from neutral loci (e.g.,
404 microsatellites, now easily available for many species) and can be sampled noninvasively
405 (e.g., from shed hair or faces, Taberlet & Luikart 1999; Broquet et al. 2007). The only
406 demographic information required is the size of local populations, which can be obtained

from basic field (e.g., mark-recapture) observations. Finally, the negative effects of both drift load (fixed deleterious mutations) and inbreeding load (segregating deleterious mutations) are accounted for, whereas empirical methods relying on the estimation of the number of lethal equivalents (Morton et al. 1956) only consider the later. Given that small populations might already be inbred to some degree, they are likely to have lost part of their standing variation and fixed part of their mutation load. We hope our study will help clarify the effects of spatial structure and connectivity on viability prospects of fragmented populations and provide additional tools to evaluate extinction threats for endangered populations.

ACKNOWLEDGMENTS

We thank M. Whitlock and T. Broquet for helpful discussions and valuable comments on a previous draft of this manuscript. The Swiss National Fund provided financial support (grants 3100A0-108100 to N.P. and PBLAA-109652 and PA00A-115383 to F.G). The simulations were run on WestGrid (www.westgrid.ca).

LITERATURE CITED

Bataillon, T., and M. Kirkpatrick. 2000. Inbreeding depression due to mildly deleterious mutations in finite populations: size does matter. Genetical Research **75**:75-81.

Broquet, T., N. Menard, and E. Petit. 2007. Noninvasive population genetics: a review of sample source, diet, fragment length and microsatellite motif effects on amplification success and genotyping error rates. Conservation Genetics **8**:249-260.

Bush, J. W. 2006. Heterosis in an isolated, effectively small, and self-fertilizing population of

the flowering plant *Leavenworthia alabamica*. Evolution **60**:184-191.

Caballero, A., and P. D. Keightley. 1994. A pleiotropic nonadditive model of variation in quantitative traits. Genetics **138**:883-900.

Coulson, T. N., J. M. Pemberton, S. D. Albon, M. Beaumont, T. C. Marshall, J. Slate, F. E. Guinness, and T. H. Clutton-Brock. 1998. Microsatellites reveal heterosis in red deer. Proceedings of the Royal Society of London Series B-Biological Sciences **265**:489-495.

Couvet, D. 2002. Deleterious effects of restricted gene flow in fragmented populations. Conservation Biology **16**:369-376.

Duarte, L.C., C. Bouteiller, P. Fontanillas, E. Petit, and N. Perrin. 2003. Inbreeding in the greater white-toothed shrew *Crocidura russula*. Evolution **5**:638-645.

Eckstein, R. L., R. A. O'Neill, J. Danihelka, A. Otte, and W. Kohler. 2006. Genetic structure among and within peripheral and central populations of three endangered floodplain violets. Molecular Ecology **15**:2367-2379.

Frankel, O. H., and M. E. Soulé. 1981. Conservation and evolution. Cambridge University Press, Cambridge, United Kingdom.

Frankham, R. 1995. Conservation genetics. Annual Review of Genetics **29**:305-327.

Glémin, S. 2003. How are deleterious mutations purged? Drift versus nonrandom mating. Evolution **57**:2678-2687.

Guillaume, F., and J. Rougemont. 2006. Nemo: an evolutionary and population genetics programming framework. Bioinformatics **22**:2556-2557.

450 Hanski, I., and O. Ovaskainen. 2000. The metapopulation capacity of a fragmented landscape.
451 Nature **404**:755-758.

452 Higgins, K., and M. Lynch. 2001. Metapopulation extinction caused by mutation
453 accumulation. Proceedings of the National Academy of Sciences of the United States
454 of America **98**:2928-2933.

455 IUCN (World Conservation Union). 2001. IUCN red list categories and criteria. Version 3.1.
456 IUCN Species Survival Commission, Gland, Switzerland, and Cambridge, United
457 Kingdom.

458 Kalinowski, S. T., and P. W. Hedrick. 1998. An improved method for estimating inbreeding
459 depression in pedigrees. Zoo Biology **17**:481-497.

460 Kawamura, K., M. Kubota, M. Furukawa, and Y. Harada. 2007. The genetic structure of
461 endangered indigenous populations of the amago salmon, *Oncorhynchus*
462 *masouishikawae*, in Japan. Conservation Genetics **8**:1163-1176.

463 Keller, L. F., and D. M. Waller. 2002. Inbreeding effects in wild populations. Trends in
464 Ecology & Evolution **17**:230-241.

465 Keightley, P. D. 1994. The distribution of mutation effects on viability in *Drosophila-*
466 *melanogaster*. Genetics **138**:1315-1322.

467 Kimura, M., T. Maruyama, and J. F. Crow. 1963. Mutation load in small populations.
468 Genetics **48**:1303-1312.

469 Kruuk, L. E. B., B. C. Sheldon, and J. Merila. 2002. Severe inbreeding depression in collared
470 flycatchers (*Ficedula albicollis*). Proceedings of the Royal Society of London Series

B-Biological Sciences **269**:1581-1589.

Lacy, R. C., and D. B. Lindenmayer. 1995. A simulation study of the impacts of population subdivision on the mountain brushtail possum *Trichosurus caninus* Ogilby (Phalangeridae, Marsupialia) in South-Eastern Australia. 2. Loss of genetic-variation within and between subpopulations. Biological Conservation **73**:131-142.

Lande, R. 1993. Risks of population extinction from demographic and environmental stochasticity and random catastrophes. The American Naturalist **142**:911-927.

Lande, R. 1994. Risks of population extinction from new deleterious mutations. Evolution **48**:1460-1469.

Lande, R. 1995. Mutation and conservation. Conservation Biology **9**:782-791.

Loewe, L., and B. Charlesworth. 2006. Inferring the distribution of mutational effects on fitness in *Drosophila*. Biology Letters **2**:426-430.

Lynch, M., J. Conery, and R. Burger. 1995. Mutation accumulation and the extinction of small populations. The American Naturalist **146**: 489-518.

Lynch, M., J. Blanchard, D. Houle, T. Kibota, S. Schultz, L. Vassilieva, and J. Willis. 1999. Perspective: Spontaneous deleterious mutation. Evolution **53**:645-663.

Madsen, T., B. Stille, and R. Shine. 1996. Inbreeding depression in an isolated population of adders *Vipera berus*. Biological Conservation **75**:113-118.

Marr, A. B., L. F. Keller, and P. Arcese. 2002. Heterosis and outbreeding depression in descendants of natural immigrants to an inbred population of song sparrows (*Melospiza melodia*). Evolution **56**:131-142.

492 Mills, L. S., and F. W. Allendorf. 1996. The one-migrant-per-generation rule in conservation
493 and management. Conservation Biology **10**:1509-1518.

494 Morjan, C. L., and L. H. Rieseberg. 2004. How species evolve collectively: implications of
495 gene flow and selection for the spread of advantageous alleles. Molecular Ecology
496 **13**:1341-1356.

497 Morton, N. E., J. F. Crow, and H. J. Muller. 1956. An estimate of the mutational damage in
498 man from data on consanguineous marriages. Proceedings of the National Academy of
499 Sciences of the United States of America **42**:855-863.

500 Mukai, T., Chigusa, S. I., Mettler, L. E., and J. F. Crow, J. F. 1972. Mutation rates and
501 dominance of genes affecting viability in *Drosophila melanogaster*. Genetics **72**: 335-
502 355.

503 Nei, M., and R. K. Chesser. 1983. Estimation of fixation indexes and gene diversities. Annals
504 of Human Genetics **47**:253-259.

505 Newman, D., and D. Pilson. 1997. Increased probability of extinction due to decreased
506 genetic effective population size: Experimental populations of *Clarkia pulchella*.
507 Evolution **51**:354-362.

508 Phadnis, N., and J. D. Fry. 2005. Widespread correlations between dominance and
509 homozygous effects of mutations: Implications for theories of dominance. Genetics
510 **171**:385-392.

511 Ralls, K., J. D. Ballou, and A. Templeton. 1988. Estimates of lethal equivalents and the cost
512 of inbreeding in mammals. Conservation Biology **2**:185-193.

513 Reed, D. H. 2005. Relationship between population size and fitness. Conservation Biology
514 **19**:563-568.

515 Reed, D. H., A. C. Nicholas, and G. E. Stratton. 2007. Inbreeding levels and prey abundance
516 interact to determine fecundity in natural populations of two species of wolf spider.
517 Conservation Genetics **8**:1061-1071.

518 Rowe, G., T. J. C. Beebee, and T. Burke. 2000. A microsatellite analysis of natterjack toad,
519 *Bufo calamita*, metapopulations. Oikos **88**:641-651.

520 Saccheri, I., M. Kuussaari, M. Kankare, P. Vikman, W. Fortelius, and I. Hanski. 1998.
521 Inbreeding and extinction in a butterfly metapopulation. Nature **392**:491-494.

522 Simmons, M. J., and J. F. Crow. 1977. Mutations affecting fitness in *Drosophila* populations.
523 Annual Review of Genetics **11**:49-78.

524 Spielman, D., B. W. Brook, and R. Frankham. 2004. Most species are not driven to extinction
525 before genetic factors impact them. Proceedings of the National Academy of Sciences
526 of the United States of America **101**:15261-15264.

527 Taberlet, P., and G. Luikart. 1999. Non-invasive genetic sampling and individual
528 identification. Biological Journal of the Linnean Society **68**:41-55.

529 Theodorou, K., and D. Couvet. 2006. Genetic load in subdivided populations: interactions
530 between the migration rate, the size and the number of subpopulations. Heredity
531 **96**:69-78.

532 Wang, J. L. 2004. Application of the one-migrant-per-generation rule to conservation and
533 management. Conservation Biology **18**:332-343.

534 Wang, J. L., W. G. Hill, D. Charlesworth, and B. Charlesworth. 1999. Dynamics of
535 inbreeding depression due to deleterious mutations in small populations: mutation
536 parameters and inbreeding rate. Genetical Research **74**:165-178.

537 Whitlock, M. C. 1992. Temporal fluctuations in demographic parameters and the genetic
538 variance among populations. Evolution **46**:608-615.

539 Whitlock, M. C. 2002. Selection, load and inbreeding depression in a large metapopulation.
540 Genetics **160**:1191-1202.

541 Whitlock, M. C. 2003. Fixation probability and time in subdivided populations. Genetics
542 **164**:767-779.

543 Whitlock, M. C., and D. E. McCauley. 1999. Indirect measures of gene flow and migration:
544 F_{ST} not equal 1/(4Nm + 1). Heredity **82**:117-125.

545 Whitlock, M. C., P. K. Ingvarsson, and T. Hatfield. 2000. Local drift load and the heterosis of
546 interconnected populations. Heredity **84**:452-457.

547 TABLES

548 **Table 1**. Spearman rank correlations between the variables used as predictor of offspring
549 viability and median time to extinction (MTE).

	Log(N)[a]	Log(d)[b]	Log(1-F_{ST})[c]	Log(H_O)[d]	Log(H_S)[e]	H_T[f]
Log(N_t)[g]	0.003	0.58	-0.12	0.35	0.35	0.53
Log(N)		-0.80	0.66	0.52	0.55	-0.55
Log(d)			-0.60	-0.22	-0.24	0.76
Log(1-F_{ST})				0.75	0.77	-0.87
Log(H_O)					0.97	-0.43
Log(H_S)						-0.44

[a] N = local population size, [b] d = number of demes, [c] F_{ST} = genetic structure, [d] H_O = observed heterozygosity, [e] H_S = within deme expected heterozygosity, [f] H_T = expected heterozygosity, [g] N_t = total metapopulation size.

551 **Table 2**. Regression models for offspring viability as a function of F_{ST} and H_S for the

552 different data sets.[a]

Dataset [b]	Parameters [c]	Mating system and migration model [d]	Intercept	Log(1-F_{ST})		Log(H_S)		Total R^2	Rank
				Coef.	R^2	Coef.	R^2		
1	*f*=15, *U*=0.5, exponential	IM-random mating	0.903	0.543	0.41-0.54	0.442	0.36-0.49	0.90	1
2	*f*=15, *U*=0.5, exponential	IM-polygyny	1.411	0.598	0.46-0.51	0.678	0.43-0.48	0.94	1
3	*f*=15, *U*=0.5, exponential	IM-selfing	1.548	0.606	0.45-0.63	0.518	0.28-0.46	0.91	1
4	*f*=15, *U*=0.5, exponential	SSM-random mating	1.133	0.319	0.27-0.41	0.573	0.51-0.65	0.92	1
5	*f*=15, *U*=0.5, exponential	SSM-polygyny	1.877	0.380	0.31-0.40	0.903	0.57-0.65	0.97	1
6	*f*=15, *U*=0.5, exponential	SSM-selfing	1.976	0.381	0.26-0.57	0.726	0.36-0.67	0.93	1
1-3	*f*=15, *U*=0.5, exponential	IM	1.114	0.529	0.32-0.45	0.468	0.25-0.39	0.71	1
4-6	*f*=15, *U*=0.5, exponential	SSM	1.414	0.322	0.19-0.40	0.629	0.34-0.54	0.74	1
1, 4	*f*=15, *U*=0.5, exponential	Random mating	0.948	0.384	0.30-0.46	0.485	0.41-0.56	0.87	1
2, 5	*f*=15, *U*=0.5, exponential	Polygyny	1.494	0.460	0.36-0.47	0.737	0.50-0.56	0.92	1
3, 6	*f*=15, *U*=0.5, exponential	Selfing	1.645	0.454	0.33-0.59	0.585	0.30-0.56	0.88	1
1-6	*f*=15, *U*=0.5, exponential	All data pooled	1.185	0.391	0.24-0.42	0.523	0.28-0.46	0.70	1
7	*f*=6, *U*=0.5, exponential	IM-random mating	0.689	0.342	0.20-0.25	0.326	0.59-0.64	0.85	5
8	*f*=15, *U*=1, exponential	IM-random mating	-0.395	0.483	0.46-0.50	0.358	0.43-0.48	0.93	2
9	*f*=15, *U*=0.5, log-normal	IM-random mating	0.905	0.480	0.41-0.59	0.419	0.36-0.54	0.95	1
10	*f*=15, *U*=0.5, gamma	IM-random mating	0.798	0.516	0.49-0.61	0.323	0.26-0.38	0.87	1

[a] Also shown are the intercept, the regression coefficients and the variance explained by F_{ST} and H_S, the total amount of variance explained, and the model ranking. Because order of introduction of variables in the model affects the amount of explained variance (but not the regression coefficients), partial R^2 is shown for each variable when introduced first and second. Significance levels of all coefficients and R^2 are below 0.0001.

[b] Each dataset is assigned a number (1 to 10). When regressions were performed on pooled data, the datasets used are shown.

[c] Shown are the fecundity values (per female), the genomic mutation rate and the type of distribution for the deleterious effects.

[d] "IM" stands for "Island migration model" and "SSM" for "Stepping-stone migration model". "IM-random mating" means that all simulations run with random mating and island migration model were used in the regression (but with the same parameter values). "IM" means that all simulations run under island migration model with the same parameter values were pooled (independently of the mating system) and "Random mating" that all simulations run under random mating with the same parameter value were pooled (independently of the migration model). "All data pooled" means that all simulations run with the same parameters values were pooled (independently of the mating system and migration model).

553 **Table 3.** Regression models for median time to extinction as a function of *Hs* and local

554 population sizes for the different data sets.[a]

Dataset [b]	Parameters [c]	Mating system and migration model [d]	Intercept	Log(H_S)		Log(N)		Total R^2	Rank
				Coef.	R^2	Coef.	R^2		
1	f=15, U=0.5, exponential	IM-random-mating	$2.40 \cdot 10^{-03}$	$-8.83 \cdot 10^{-04}$	0.13-0.46	$-1.42 \cdot 10^{-03}$	0.38-0.71	0.84	3
2	f=15, U=0.5, exponential	IM-polygyny	$2.21 \cdot 10^{-03}$	$-8.41 \cdot 10^{-04}$	0.9-0.31	$-1.17 \cdot 10^{-03}$	0.49-0.70	0.79	3
3	f=15, U=0.5, exponential	IM-selfing	$-1.08 \cdot 10^{-03}$	$-1.09 \cdot 10^{-03}$	0.39-0.76	$-6.64 \cdot 10^{-04}$	0.17-0.54	0.93	2
4	f=15, U=0.5, exponential	SSM-random-mating	$-5.75 \cdot 10^{-04}$NS	$-1.20 \cdot 10^{-03}$	0.25-0.83	$-8.51 \cdot 10^{-04}$	0.12-0.70	0.95	2
5	f=15, U=0.5, exponential	SSM-polygyny	$-1.11 \cdot 10^{-03}$	$-1.23 \cdot 10^{-03}$	0.26-0.79	$-6.76 \cdot 10^{-04}$	0.14-0.67	0.93	1
6	f=15, U=0.5, exponential	SSM-selfing	$-2.66 \cdot 10^{-03}$	$-1.15 \cdot 10^{-03}$	0.50-0.94	$-2.89 \cdot 10^{-04}$	0.3-0.46	0.97	2
1-3	f=15, U=0.5, exponential	IM	$1.30 \cdot 10^{-03}$	$-8.73 \cdot 10^{-04}$	0.16-0.30	$-9.85 \cdot 10^{-04}$	0.36-0.51	0.66	1
4-6	f=15, U=0.5, exponential	SSM	$-1.34 \cdot 10^{-03}$	$-1.15 \cdot 10^{-03}$	0.32-0.70	$-5.61 \cdot 10^{-04}$	0.10-0.48	0.81	2
1, 4	f=15, U=0.5, exponential	Random mating	$2.16 \cdot 10^{-03}$	$-7.71 \cdot 10^{-04}$	0.13-0.52	$-1.29 \cdot 10^{-03}$	0.32-0.71	0.84	3
2, 5	f=15, U=0.5, exponential	Polygyny	$1.43 \cdot 10^{-03}$	$-8.55 \cdot 10^{-04}$	0.13-0.48	$-9.83 \cdot 10^{-04}$	0.34-0.68	0.81	2
3, 6	f=15, U=0.5, exponential	Selfing	$-1.06 \cdot 10^{-03}$	$-8.95 \cdot 10^{-04}$	0.36-0.73	$-5.72 \cdot 10^{-04}$	0.13-0.50	0.86	2
1-6	f=15, U=0.5, exponential	All data pooled	$7.65 \cdot 10^{-04}$	$-8.36 \cdot 10^{-04}$	0.19-0.43	$-8.30 \cdot 10^{-04}$	0.25-0.49	0.68	1
7	f=6, U=0.5, exponential	IM-random mating	$8.53 \cdot 10^{-03}$	$-5.95 \cdot 10^{-04}$	0.04-0.08	$-2.49 \cdot 10^{-03}$	0.65-0.69	0.73	3
8	f=15, U=1, exponential	IM-random mating	$4.47 \cdot 10^{-03}$	$-1.43 \cdot 10^{-03}$	0.12-0.35	$-1.91 \cdot 10^{-03}$	0.38-0.61	0.73	4
9	f=15, U=0.5, log-normal	IM-random mating	$5.56 \cdot 10^{-04}$	$-3.59 \cdot 10^{-03}$	0.21-0.51	$-4.88 \cdot 10^{-04}$	0.38-0.68	0.89	3
10	f=15, U=0.5, gamma	IM-random mating	$3.82 \cdot 10^{-03}$	$-7.49 \cdot 10^{-04}$	0.09-0.45	$-1.75 \cdot 10^{-03}$	0.49-0.85	0.94	3

[a] Also shown are the intercept, the regression coefficients and the explained variance by H_S and local population size (N), the total amount of variance explained, and the model ranking. Because order of introduction of variables in the model affects the amount of explained variance (but not the regression coefficients), partial R^2 is shown for each variable when introduced first and second. Significance levels of slope coefficients and R^2 are below 0.01. For the intercept, p-values < 0.025 but one case noted NS.

[b] Each dataset is assigned a number (1 to 10). When regressions were performed on pooled data, the datasets used are shown.

[c] Shown are the fecundity values (per female), the genomic mutation rate and the type of distribution for the deleterious effects.

[d] "IM" stands for "Island migration model" and "SSM" for "Stepping-stone migration model". "IM-random mating" means that all simulations run with random mating and island migration model were used in the regression (but with the same parameter values). "IM" means that all simulations run under island migration model with the same parameter values were pooled (independently of the mating system) and "Random mating" that all simulations run under random mating with the same parameter value were pooled (independently of the migration model). "All data pooled" means that all simulations run with the same parameters values were pooled (independently of the mating system and migration model).

555 **FIGURE LEGENDS**

556 **Figure 1.** Offspring viability as a function of genetic differentiation (F_{ST}) and within-
557 population heterozygosity (H_S) for simulations performed under (a) polygyny (datasets 2 and
558 5), (b) random mating (datasets 1 and 4), and (c) selfing (datasets 3 and 6). Dots indicate
559 viable metapopulations, lighter symbols signalling higher offspring viability. The expected
560 isoclines for viability (lines) are calculated from the regression models in Table 2. Crosses
561 represent simulations that crashed before generation 5000. Data points corresponding to the
562 same total metapopulation size are aligned on the different curves

563 **Figure 2.** Median time to extinction (MTE) as a function of within-population heterozygosity
564 (H_S) and population sizes (N) for simulations performed under (a) polygyny (datasets 2 and
565 5), (b) random mating (datasets 1 and 4), and (c) selfing (datasets 3 and 6) (x- and y-axes are
566 log transformed for graphical presentation). Dots indicate metapopulations that collapsed,
567 lighter symbols signalling longer time to extinction. The expected isoclines for MTE (lines)
568 are calculated with the coefficients of the regression models in Table 3. Crosses represent
569 simulations that survived at least until generation 5000.

570 **Figure 3.** Offspring viability as a function of effective migration rate N_m (log scale) for (a)
571 polygyny (datasets 2 and 5) , (b) selfing (datasets 3 and 6), (c) random mating, pooling all 3
572 distribution models for deleterious effects (datasets 1,4, 9 and 10), (d) random mating with
573 lowered fecundity (f=6, dataset 7), and (e) random mating with increased genomic mutation
574 rate (U=1, dataset 8). A viability of zero is assigned to simulations that crashed, which
575 occurred whenever viability decreased below a threshold value (about 0.2 for f=15, and 0.4
576 for f=6). When effective migration rates exceeded 1 (vertical line), extinctions occurred only
577 at low metapopulation sizes (N_t=200, crosses) but never at larger sizes (open circles).

FIGURES

Figure 1

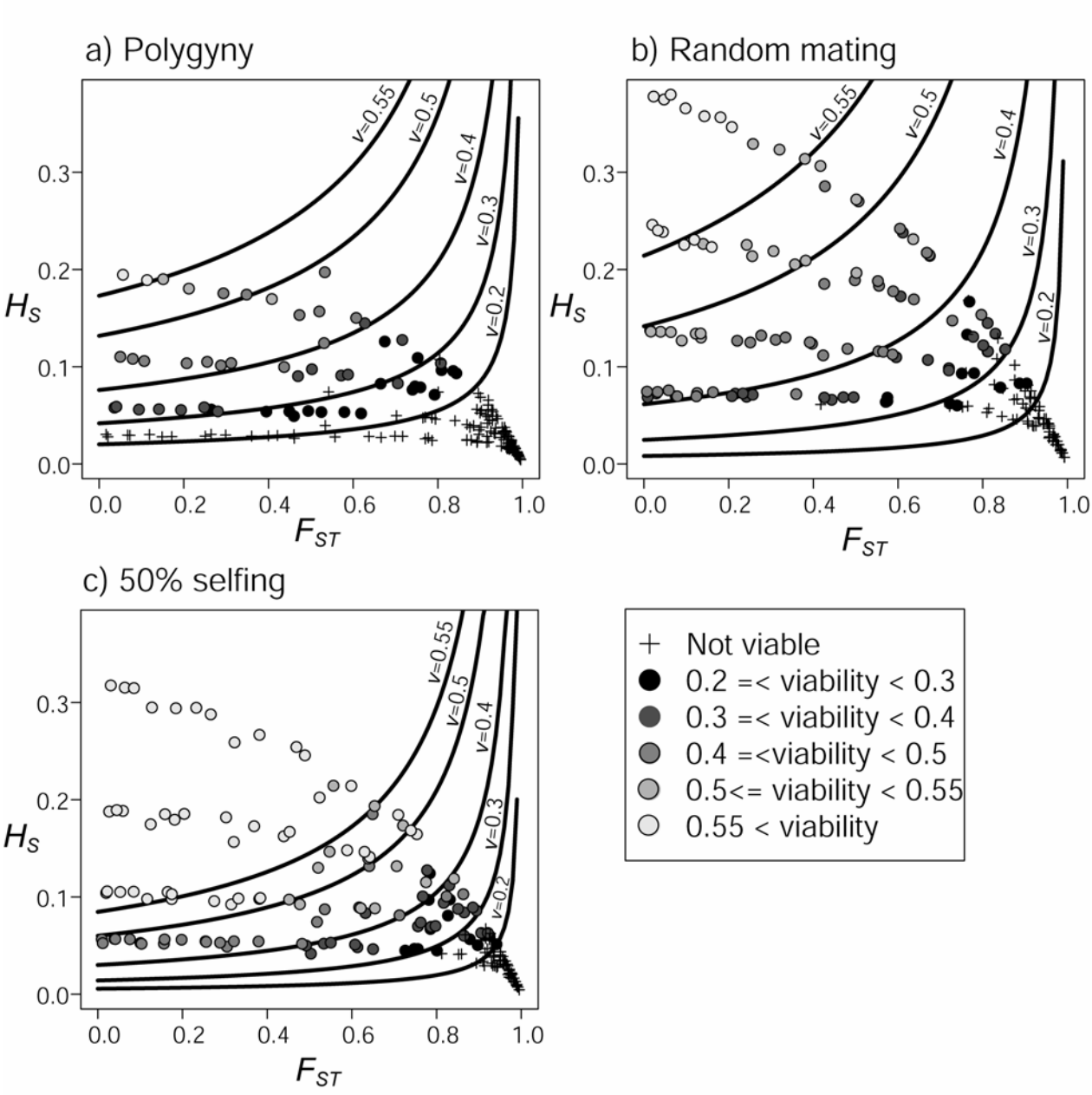

Figure 2

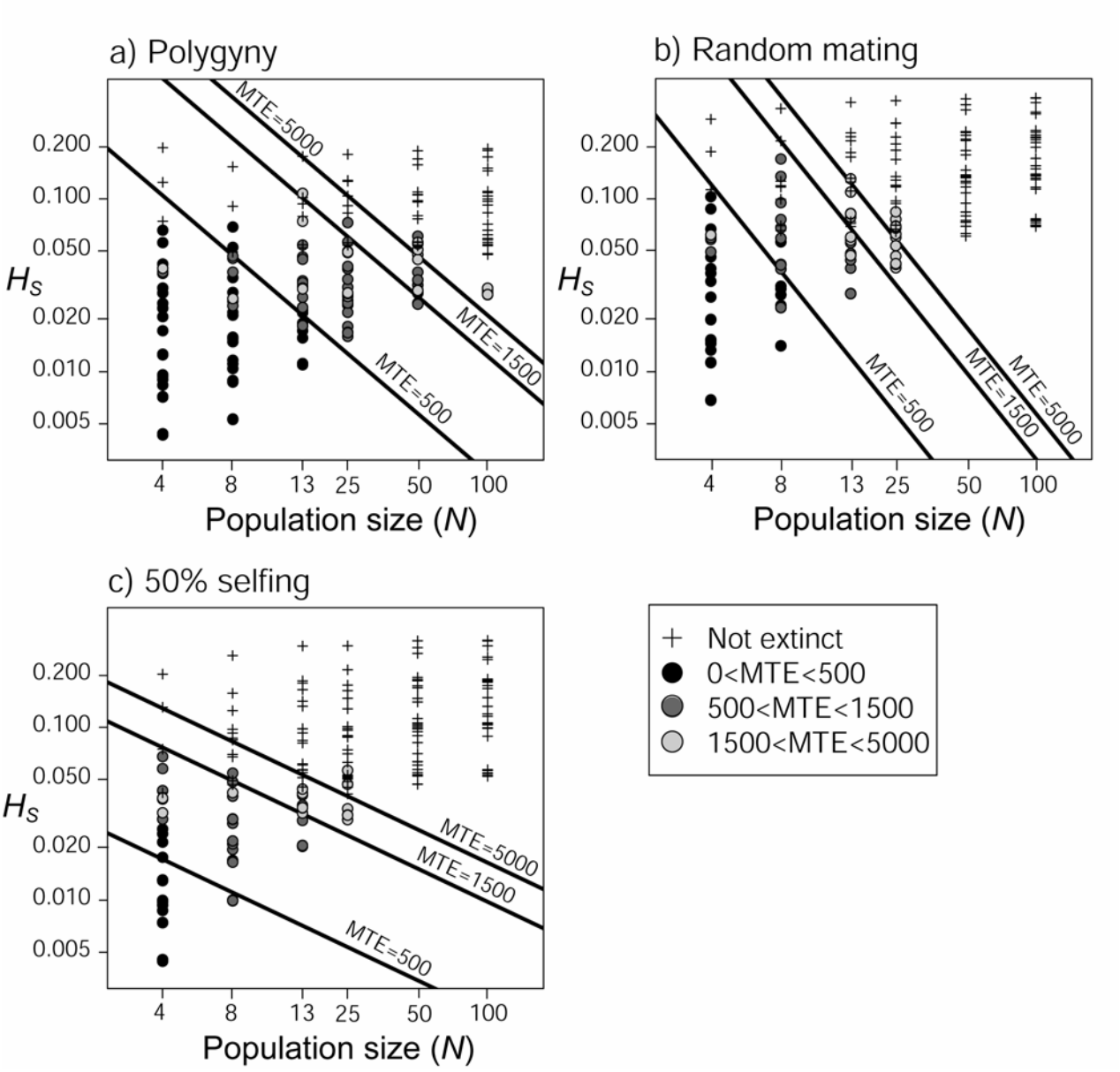
a) Polygyny
b) Random mating
c) 50% selfing
H_S
0.200
0.100
0.050
0.020
0.010
0.005
4
8
13
25
50
100
Population size (N)
MTE=5000
MTE=1500
MTE=500
Not extinct
0<MTE<500
500<MTE<1500
1500<MTE<5000

Figure 3

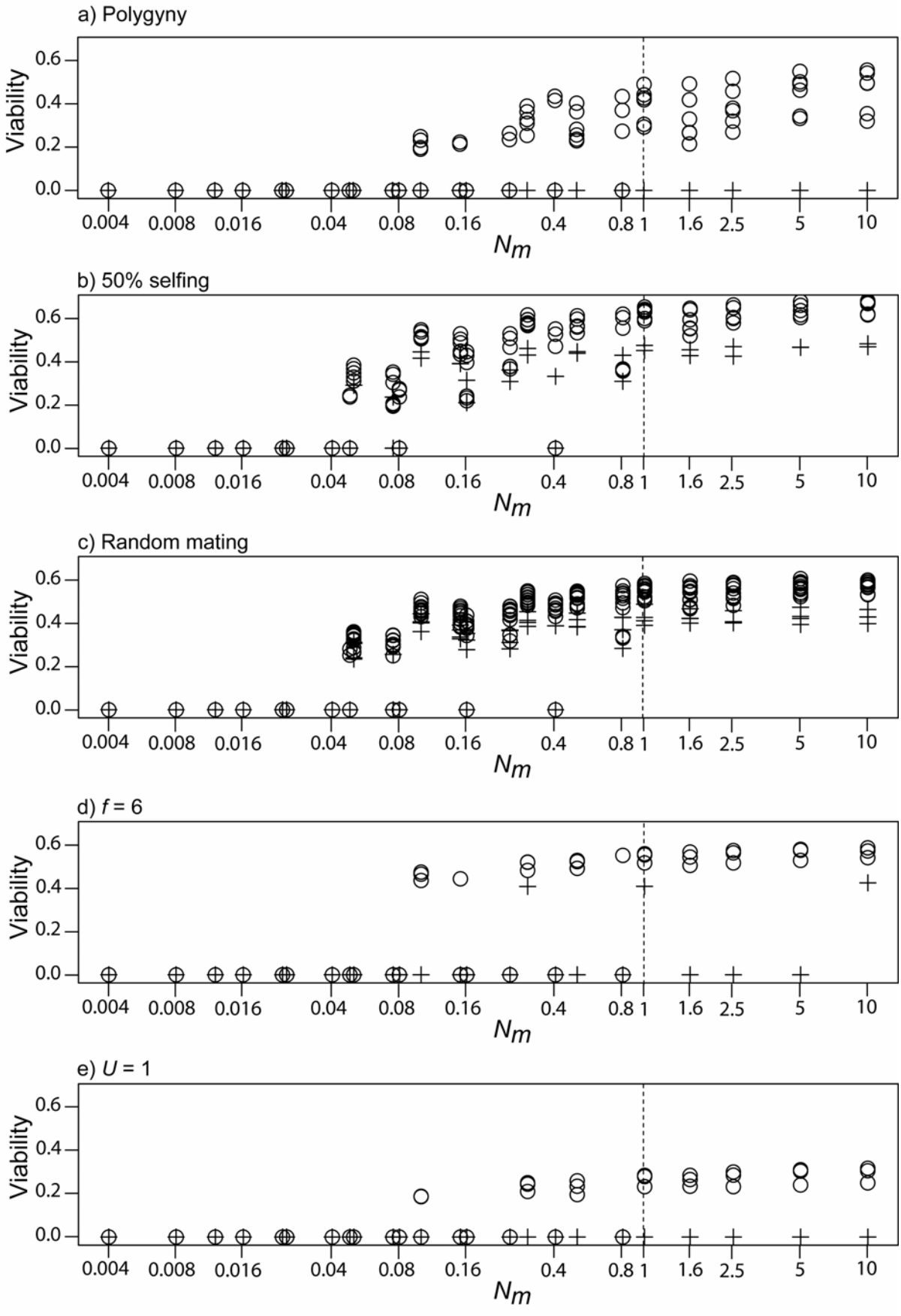
a) Polygyny
b) 50% selfing
c) Random mating
d) f = 6
e) U = 1
Viability
0.0
0.2
0.4
0.6
0.004
0.008
0.016
0.04
0.08
0.16
0.4
0.8
1
1.6
2.5
5
10
Nm